Available online at www.sciencedirect.com
SCIENCE DIRECT®
Bioorganic & Medicinal Chemistry 13 (2005) 4544–4551
Bioorganic & Medicinal Chemistry

Understanding human 15-hydroxyprostaglandin dehydrogenase binding with NAD^+ and PGE_2 by homology modeling, docking and molecular dynamics simulation

Adel Hamza,[a,†] Hoon Cho,[a,b,†] Hsin-Hsiung Tai[a,*] and Chang-Guo Zhan[a,*]

[a]*Department of Pharmaceutical Sciences, College of Pharmacy, University of Kentucky, Lexington, KY 40536, USA*
[b]*College of Engineering, Chosun University, Gwangju 501-759, South Korea*

Received 25 February 2005; revised 13 April 2005; accepted 13 April 2005
Available online 23 May 2005

Abstract—Homology modeling, molecular docking, and molecular dynamics simulation have been performed to determine human 15-hydroxyprostaglandin dehydrogenase (15-PGDH) binding with its NAD^+ cofactor and prostaglandin E2 (PGE_2) substrate. The computational studies have led to a three-dimensional (3D) model of the entire 15-PGDH–NAD^+–PGE_2 complex, demonstrating the detailed binding of PGE_2 with 15-PGDH for the first time. This 3D model shows specific interactions of the protein with the cofactor and substrate in qualitative agreement with available experimental data. Our model demonstrates the PGE_2-binding cavity of the protein for the first time. The model further leads to an interesting prediction that the catalytic activity of 15-PGDH should also significantly be affected by Gln148, in addition to the previously known three catalytic residues (Ser138, Tyr151, and Lys155). The reported 3D model of 15-PGDH–NAD^+–PGE_2 complex might be valuable for future rational design of novel inhibitors of 15-PGDH.

1. Introduction

Prostaglandins are derived from arachidonic acid through the prostaglandin endoperoxide synthase pathway.[1] Prostaglandins have a variety of biological activities and are relatively short-lived in vivo. A cytosolic enzyme, NAD^+-dependent 15-hydroxyprostaglandin dehydrogenase (15-PGDH), is the key catabolic enzyme, which controls the biological activities of the prostaglandins. The enzyme 15-PGDH catalyzes the oxidation of 15 (*S*)-hydroxyl group of prostaglandins to 15 ketone, resulting in the biological inactivation of prostaglandins.[2]

15-PGDH is found in most of the mammalian tissues. The highest activities are detected in lung, kidney, and placenta.[3] 15-PGDH was proposed to be a dimer composed of identical subunits with a molecular weight of 29 kDa; however, recent evidence suggests that 15-PGDH may be monomeric in its native form.[4] The cDNA of the enzyme was cloned[5] and the amino acid sequence analysis showed that 15-PGDH belongs to the short-chain dehydrogenase family, which includes more than 60 different enzymes.[6] These enzymes show a considerable diversity in their use of substrates. A comparison of the amino acid sequence of 15-PGDH with those of other short-chain dehydrogenases reveals an overall homology of 20% with several strictly conserved amino acid residues. One of us demonstrated that Tyr151, Lys155, and Ser138 of human 15-PGDH are critical for the catalytic activity and proposed that these three residues form a catalytic triad.[7–9]

Although no three-dimensional (3D) X-ray crystal structure of 15-PGDH has been reported in the literature, 3D X-ray crystal structures of the binary and tertiary complexes of another short-chain dehydrogenase 7α-hydroxysteroid dehydrogenase from *E. coli* have been elucidated.[10] These studies indicated that the hydroxyl groups of a serine (Ser138 in 15-PGDH) and a tyrosine (Tyr151 in 15-PGDH) within the active site most likely interact with the oxygen atom of the hydroxyl group of the substrate undergoing oxidation in the productive binding mode. The ε-amino group of the lysine residue forms a hydrogen bond with the *cis*-diol of the nicotinamide ribose of the coenzyme, NAD^+. It has also been

Keywords: 15-Hydroxyprostaglandin dehydrogenase; NAD^+; PGE_2; Molecular modeling; Molecular dynamics.
* Corresponding authors. Tel.: +1 8593 233943; fax: +1 8592 577585; e-mail: zhan@uky.edu
† These authors contributed equally to this study.

0968-0896/$ - see front matter © 2005 Elsevier Ltd. All rights reserved.
doi:10.1016/j.bmc.2005.04.053

found that Cys182 of human 15-PGDH is essential as this residue may form part of the NAD^+ binding domain.[11] Recently, we have demonstrated that Thr188 of human 15-PGDH appears to be critical for interaction with NAD^+ as the Thr188Ser mutant of 15-PGDH exhibited a 100-fold increase in the K_m for NAD^+ whereas the K_m for prostaglandin E2 (PGE_2) was unchanged.[12] It has also been suggested that relatively conserved residues Ile17, Asn91, and Val186 are also involved in the interaction with NAD^+ by hydrogen bonding since some mutants at each position exhibited K_m values for NAD^+ nearly 10-fold higher than that of the wild type with much smaller change in K_m values for PGE_2.[13] However, these studies were essentially focused on the residues in the conserved domain of the enzyme binding with NAD^+. A 3D model of 15-PGDH obtained from molecular modeling studies reported by Krook et al. was also used to study the 15-PGDH binding with NAD^+.[14] However, the specific binding of 15-PGDH with PGE_2 and binding of PGE_2 with NAD^+ have not been examined in terms of 3D molecular structure.

In the present work, we have built a 3D model of the entire 15-PGDH protein by performing molecular modeling and simulation. This 3D model enables us to study the binding of 15-PGDH with PGE_2 and binding of PGE_2 with NAD^+. The simulated 3D model of the entire 15-PGDH–NAD^+–PGE_2 complex provides useful insights into the architecture of the 15-PGDH active site and the stereospecific oxidation of PGE_2. The computational results also clearly suggest that the catalytic mechanism involves an amino acid residue, which has not been mentioned in the literature.

2. Methods

2.1. Initial model of the three-dimensional (3D) structure

The amino acid sequences of the human hydroxyprostaglandin dehydrogenase [AC: 31542939] were generated from the GenBank database.[15] The search for sequence similarities with several members of the prostaglandin dehydrogenase family within the Protein Data Bank (PDB)[16] database was performed with the BLAST program.[17] The coordinates of the crystal structures of Levodione Reductase from *Corynebacterium aquaticum* [ID: 1IY8 chain A, 1.6 Å resolution][18] and Tropinone Reductase-II from *Datura stramonium* [ID: 2AE2, 2.3 Å resolution][19] were used as the templates to build the initial 15-PGDH models. Multiple-sequence alignment was performed using Homology module of InsightII (Accelrys, Inc.) and then we manually adjusted the structure to move gaps from the regions within helices and strands to those of loops. The 3D-models of the hydroxyprostaglandin dehydrogenase protein were generated using the automated homology modeling tool Modeler[20,21]/InsightII with default parameters.

2.2. Model refinement and evaluation

The best initial model obtained from the homology modeling was solvated with solvent water molecules and was roughly energy-minimized in order to make it suitable for performing molecular dynamics (MD) simulation to relax the loops and side chain (see below for the details of the MD simulation procedure). During the MD simulation, constraints with a force constant of 50 kcal mol $Å^{-2}$ were applied to the backbone atoms (N, Cα, C, and O) of the structurally conserved regions (SCR). The simulated 3D model was evaluated periodically for its stereochemical quality as well as its residue packing and atomic contacts. The program used to evaluate the modeled protein structure is Procheck.[22] The atomic contact analysis was performed by using the Whatif program[23] to identify bad packing of side chain atoms or unusual residue contacts.

2.3. Molecular docking

The geometries of NAD^+ and PGE_2 molecules were optimized by performing ab initio electronic structure calculations using the Gaussian03 program[24] at the HF/6-31G* level. The optimized geometries were used to calculate the electrostatic potentials on the molecular surfaces at the same HF/6-31G* level. The calculated electrostatic potentials were used to determine the partial atomic charges by using the standard restrained electrostatic potential (RESP) fitting procedure.[25] The determined RESP charges were used in the calculations of electrostatic energy terms in the docking and MD simulation processes. The NAD^+ was added to the refined 3D model of 15-PGDH by superimposition of our 15-PGDH model with the aforementioned X-ray crystal structure complexed with NAD^+.[18] This 3D model of the 15-PGDH–NAD^+ complex was used to study further binding with substrate PGE_2 by using a molecular dynamics docking approach. In modeling the entire 15-PGDH–NAD^+–PGE_2 complex, the first step was a visual analysis of the 15-PGDH–NAD^+ complex in order to identify a suitable location (binding pocket) and orientation on the protein surface where ligand PGE_2 could have appropriate interactions with 15-PGDH–NAD^+. Thus, several possible PGE_2-binding pockets were identified. Then, PGE_2 was positioned at 9 Å in front of each of these possible binding pockets as an initial structure for the molecular docking. Each of these initial structures was used to perform a MD simulation with implicit water using the Discover module of InsightII. During the MD simulation with implicit water, only side chains of the residues in the binding pocket was allowed to move. Then, the MD-simulated structures of the 15-PGDH–NAD^+–PGE_2 complex were neutralized and solvated with water molecules. These structures were energy-minimized until the energy derivative became less than 0.001 kcal/mol/Å. Each of the energy-minimized structure was used to perform MD simulation for 1.6 ns at 300 K.

2.4. Molecular dynamics simulation procedure

The initial geometry of 15-PGDH or 15-PGDH–NAD^+–PGE_2 structure was neutralized by adding 5 sodium counterions and was solvated in a rectangular box of TIP3P water molecules[26] with a minimum solute-wall distance of 10 Å. The counterions were added randomly

with the tleap module of Amber7 program[27] and these ions were found in water outside the protein. The solvated system was energy-minimized prior to the MD simulation. The general procedure for carrying out the MD simulations in water is similar to that used in our previously reported other computational studies.[28–32] First of all, the protein–ligand was frozen and the solvent water molecules with counterions were allowed to move during a 5000-step energy minimization with the conjugate gradient algorithm and a 10 ps MD run at $T = 300$ K. After full relaxation and the entire solvated system was energy-minimized, the system was slowly heated from $T = 10$ K to $T = 300$ K in 60 ps before the production MD simulation for 1.6 ns. The MD simulation was performed with a periodic boundary condition in the NPT ensemble at $T = 300$ K with Berendsen et al.[33] temperature coupling and constant pressure ($P = 1$ atm) with isotropic molecule-based scaling. The SHAKE algorithm[34] was applied to fix all covalent bonds containing a hydrogen atom, a time step of 2 fs was used, and the non-bond pair list was updated every 10 steps. The pressure was adjusted by isotropic position scaling. The particle mesh Ewald (PME) method[35] was used to treat long-range electrostatic interactions. A residue-based cutoff of 10 Å was applied to the non-covalent interactions. During the MD simulation, the coordinates of the simulated complex were saved every 1 ps. The simulation was performed by using the Sander module of Amber7 program. The same MD simulation procedure was also performed on another 15-PGDH–NAD^+–PGE_2 complex in which the 15-PGDH protein is a mutant, Ile17Ala. The initial structure of 15-PGDH–NAD^+–PGE_2 complex for the Ile17Ala mutant was generated by using the last snapshot of the MD-simulated 15-PGDH–NAD^+–PGE_2 complex for the wild-type 15-PGDH protein but changing the side chain of the mutated residue.

All of the computations were performed on a supercomputer (Superdome) at University of Kentucky Center for Computational Sciences and on SGI Fuel workstations and a 34-processors IBM x335 Linux cluster in our own lab.

3. Results and discussion

The amino acid sequence alignment revealed 33% identity between the human 15-PGDH and *C. aquaticum* Levodione Reductase and 23% identity between the human 15-PGDH and *D. stramonium* Tropinone Reductase (Fig. 1). The 'Whatif quality report' results summarized in Table 1 indicate that the initial 15-PGDH model

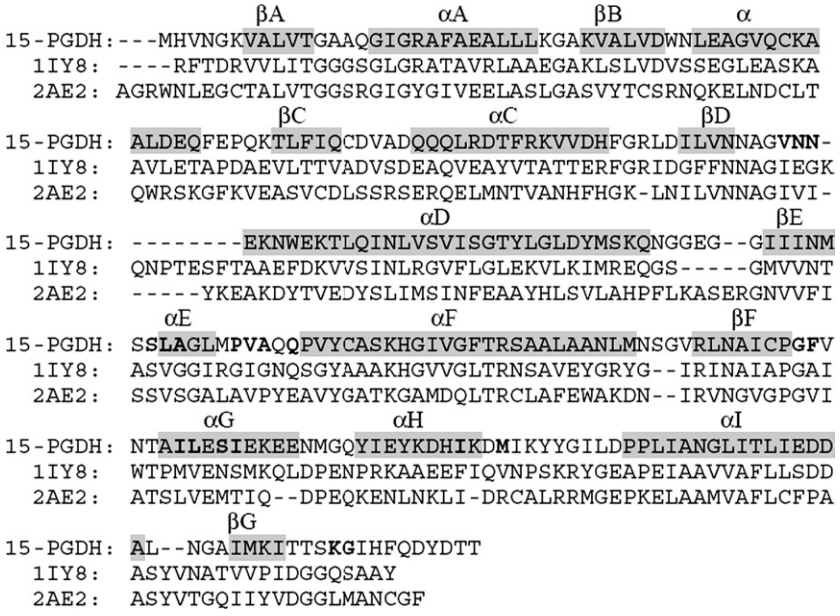

Figure 1. Multiple alignment of NAD(P)-binding Rossmann-like domain amino acid sequences. The sequences for human, *Corynebacterium aquaticum* and *Datura stramonium* were aligned using Homology module of InsightII. The secondary structures are indicated along the top of alignment (α represents α-helix; β refers to β-sheet). The residues close to PGE_2 are indicated in bold.

Table 1. Whatif quality report (*Z*-score)[a] for the initial model of 15-PGDH before performing the MD simulation and for the final model of 15-PGDH refined by the MD simulation

	Backbone–backbone contacts	Backbone–side chain contacts	Side chain–backbone contact	Side chain–side chain contacts	*Z*-score for all contacts
Initial model	1.04	−4.12	−0.36	−4.16	−2.19
Refined model	0.74	−2.90	0.21	−2.33	−1.44

[a] Whatif '*Fine Packing Quality Control*' report. Average values of the *Z*-score for all contacts of the protein can be read as follows: $-5.0 \leqslant Z$-score (guaranteed wrong structure) $< -3.0 \leqslant Z$-score (probably bad structure) $< -2.0 \leqslant Z$-score (good model).

obtained before performing the MD simulation in water is associated with a bad *Z*-score (*Z*-score less than −4) for the backbone–side chain and side chain–side chain interactions, whereas the *Z*-score of the backbone–backbone contact is positive and shows a reasonable backbone structure. The bad contacts between the side chains are usually observed when the model is built with more than one template. To fix these bad contacts, the 3D model was used to perform a MD simulation on the solvated 15-PGDH–NAD^+–PGE_2 complex. Such kind of MD simulation is usually performed for the refinement of a homology model.[36–38] Since the backbone–backbone contacts were reasonable, during the MD simulation the backbone was fixed by applying constraints on the backbone atoms as described in the METHODS section.

The analysis of the main-chain torsion angles in the refined model of 15-PGDH revealed that the 300 ps MD simulation did not cause any severe distortion of the protein backbone structure. A total of 85.6% of the residues are in the most favored regions of the Ramachandran plot with 13.9% in additionally allowed regions, giving a total of 99.5%. Other stereochemical parameters such as peptide planarity, bad non-bonded interactions, main-chain hydrogen bonding energy and standard deviations of $\chi 1$ angle (i.e., the first torsion angle of the side chain) were also examined. Moreover, the evaluation of the structural integrity of the final 15-PGDH model showed a *Z*-score of −1.44 (Table 1). The *Z*-scores calculated for individual residues are depicted in Figure 2. This value falls in the acceptable range for a valid structure. It was recommended that if the Whatif score is below −5, the model is definitely of low quality. If the Whatif value is above −2, it is recommended as a good structure.[23] The last test allowed evaluating the stability of the protein folding in the presence of NAD^+ and PGE_2. To control the stability of the simulated structure during the MD simulation, the root mean square deviation (RMSD) from the starting structure was monitored. As shown in Figure 3, the Cα RMSD stabilized near 1.7 Å indicating that the core structure of the protein was stable during the MD simulation. The simulated 3D structure model of the ternary complex of 15-PGDH–NAD^+–PGE_2 shown in Figure 4 is satisfactory, despite the low identity between the human hydroxyprostaglandin sequence and the templates.

The simulated 3D model structure of the protein consists of a core domain that includes most of the polypeptide and a small lobe (αG and αH) that protrudes from the core. A deep cleft is recognized between the core domain and small lobe, which is presumed to be the binding site for PGE_2. The center of the core domain is a seven-stranded parallel-sheet, flanked on each side by α-helices, which constitutes the 'Rossmann fold' topology. This core structure is highly conserved among the SDR family members, despite relatively low residue identity between these enzymes (around 30% identity).[6,39] The small lobe of this model is also very similar

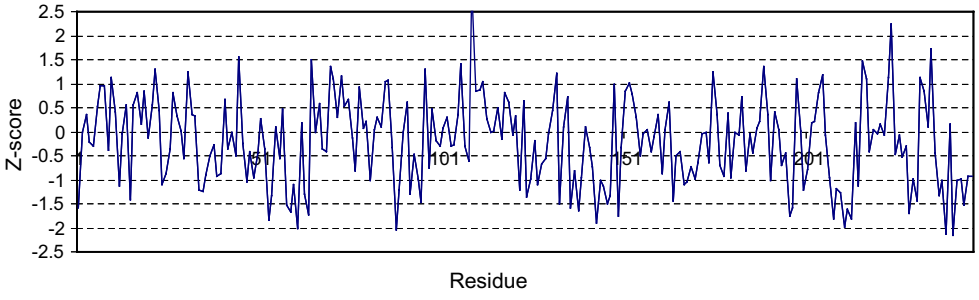

Figure 2. Whatif quality report of the human 15-PGDH model.

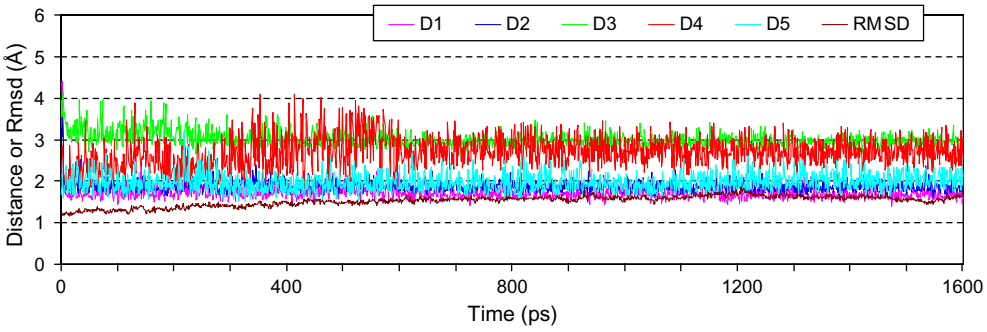

Figure 3. Internuclear distances and C_α trace RMSD during the MD simulation of the wild type with the ligands. The distances D1 to D5 are depicted in Figure 5. D1 represents the distance between the hydroxyl hydrogen of Thr188 and the phosphate oxygen of NAD^+. D2 refers to the distance between hydrogen of Ile17 backbone NH and the phosphate oxygen of NAD^+. D3 is the distance between oxygen of the sugar group of NAD^+ and nitrogen NZ atom of the amine group of Lys155. D4 represents the distance between the oxygen of the amide group of the nicotinamide ring and the main-chain amine of Val186. D5 is the distance between oxygen of Gln148 amide group and the hydroxyl hydrogen of PGE_2.

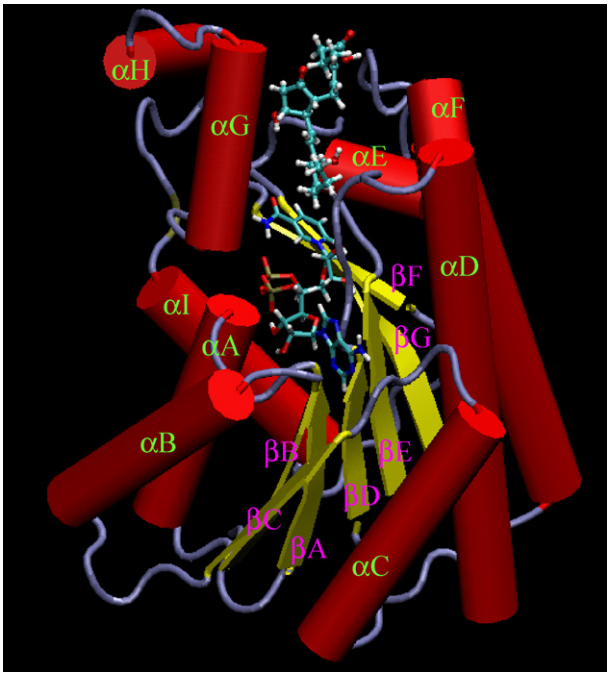

Figure 4. 3D structure of 15-PGDH–NAD^+–PGE_2 complex. PGE_2 (ball and stick), NAD^+ (stick).

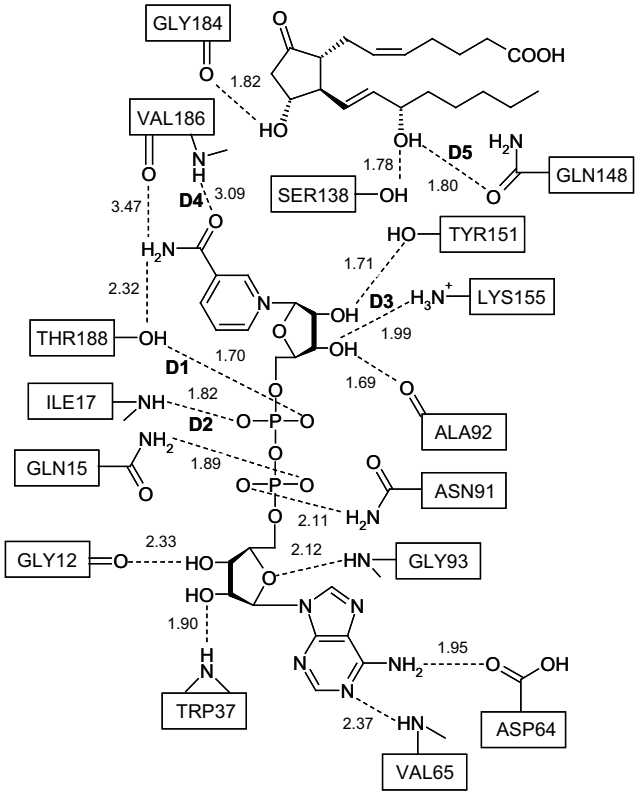

Figure 5. Schematic view of the interactions of NAD^+ and PGE_2 with 15-PGDH. The hydrogen bonds are indicated with dashed lines. The distances are given in angstroms.

to each other, although the structure of this region is highly variable among SDR family members for which a few crystal structures have been known. As seen in Figure 4, NAD^+ is located at the bottom of the cleft between the core domain and the small lobe. The carboxamide group of the nicotinamide ring is anchored by the main-chain oxygen and nitrogen atoms of Val186 and the side-chain oxygen of Thr188 (Fig. 5). This tight binding of the carboxamide to the protein directs the face of the nicotinamide ring toward the PGE_2, consistent with a C-15 hydrogen transfer.

Our simulated 3D model of the entire 15-PGDH–NAD^+–PGE_2 complex is consistent with all of the previously reported experimental data concerning the catalytic activity of 15-PGDH mutants.[7–9,12,13,40] For example, our model of the 15-PGDH–NAD^+–PGE_2 complex reveals that the NH_2 group of Asn91 side chain has a hydrogen bond with a oxygen atom of NAD^+, as seen in Figure 5, which explains why the Asn91Ala mutation decreased the catalytic activity of 15-PGDH for NAD^+ by ~12-fold. Indeed, residues Gln15, Ile17, Trp37, Asn91, Ser138, Tyr151, Val186, Lys155, and Thr188 have been postulated to be of functional importance in the specific binding of the cofactor.[13] These residues stay around NAD^+ and stabilize it through a network of hydrogen bonds. Our simulated model theoretically supports the postulation. Moreover, in our 3D model the binding cavity of the PGE_2 substrate is found to be located between αE, αF, αG, and αH helices and C-terminal residues, which is consistent with the experimental finding that the protein activity was changed when the C-terminal residues were mutated.[41]

We note that some essential residues in a long segment Ile190–Pro222 were not included in the 3D model of the human 15-PGDH reported by Krook et al.[14] Our results demonstrate that the binding pocket of PGE_2 is close to these amino acids, including Ile190 to E198 (αG helix), Tyr206 to Met213 (αH helix and loop), and others indicated in Figure 1. Based on our modeling, the bound PGE_2 is predicted to be in contact with about eight amino acids in 15-PGDH (Fig. 6). The hydroxyl groups on C-11 and C-15 of PGE_2 have hydrogen bonds with the main-chain oxygen of Gly184, the side-chain hydroxyl group of Ser138, and the side-chain oxygen of Gln148 (Fig. 5). The PGE_2 binding site is mainly surrounded by hydrophobic residues (Val145, Ala146, Gly184, Ile194, and Gly250), most of which are located in the loops within the core domain or between αE and αF.

On the basis of the previous extensive experimental studies, it has been proposed in the literature[10,13,39,41–44] that the mechanism for the reaction of PGE_2 catalyzed by 15-PGDH and other members of the SDR family involves a 'Ser-Tyr-Lys catalytic triad', which consists of Ser138, Tyr151, and Lys155 in 15-PGDH. As depicted in Figure 5, our model shows close contacts of the substrate with these three residues, which is consistent with the experimental observation that these three residues are involved in the catalytic mechanism. Our model depicted in Figure 5 further reveals for the first time that Gln148 should also have a role on the catalysis, because its side-chain oxygen atom strongly hydrogen bonds to the hydroxyl group of the substrate.

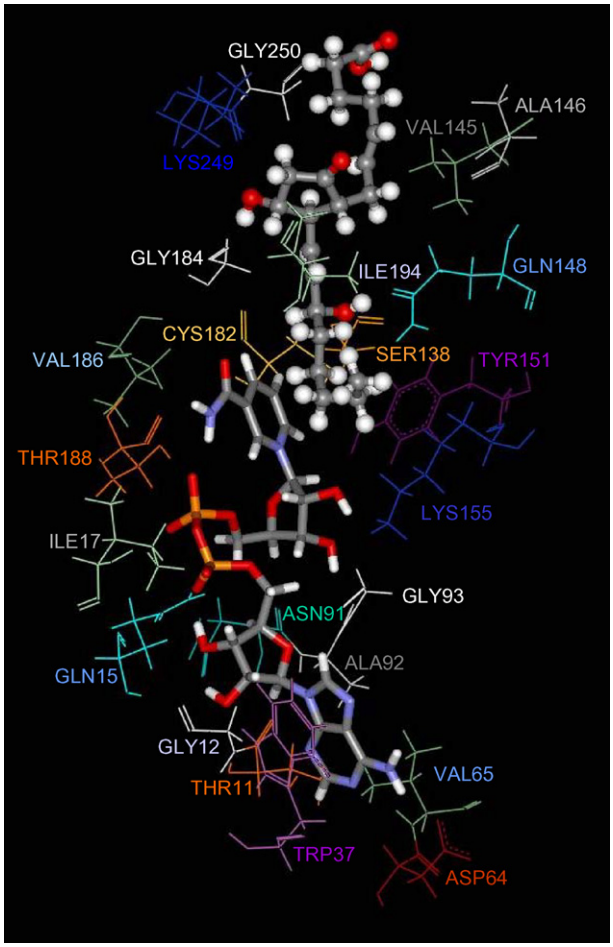

Figure 6. 3D view of the PGE_2 and NAD^+ ligands in the human 15-PGDH binding site.

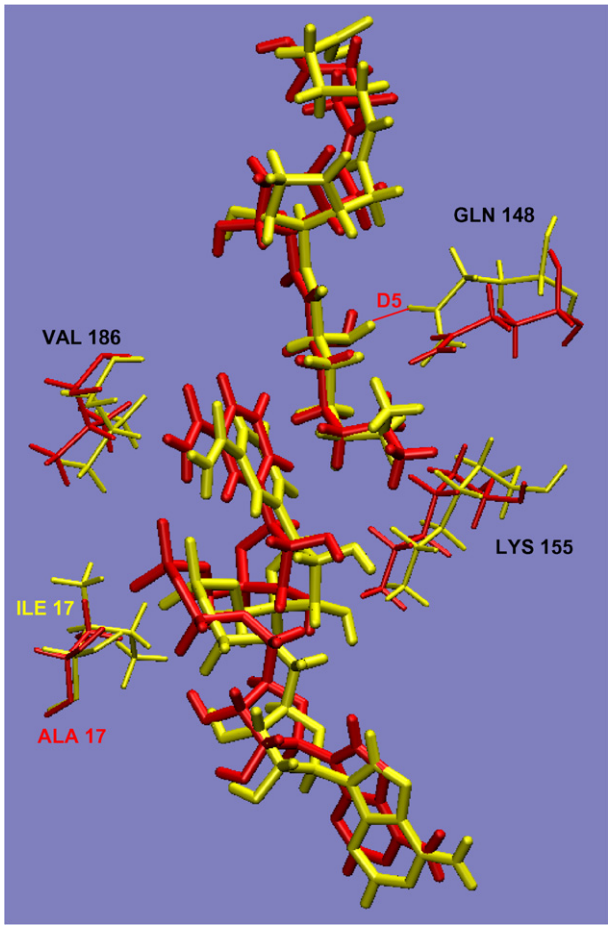

Figure 7. Relative positions of NAD^+ and PGE_2 and some residues of 15-PGDH wild-type and I17A mutant. The yellow and red refer to the wild-type and mutant complexes, respectively.

Recently reported experimental data[13] indicated that exchanging Ile17 to Ala decreased the biological activity of the resulting mutant significantly. In order to interpret such an interesting experimental finding and to confirm our simulated 3D model of 15-PGDH–NAD^+–PGE_2 complex concerning the protein–ligand interactions for 15-PGDH with NAD^+ and PGE_2, we also simulated the 15-PGDH–NAD^+–PGE_2 complex for the Ile17Ala mutant 15-PGDH. The mutated residue is shown in Figure 7. Figures 3 and 8 show that the MD trajectory of the simulated 15-PGDH–NAD^+–PGE_2 complex for the wild-type protein was stabilized after

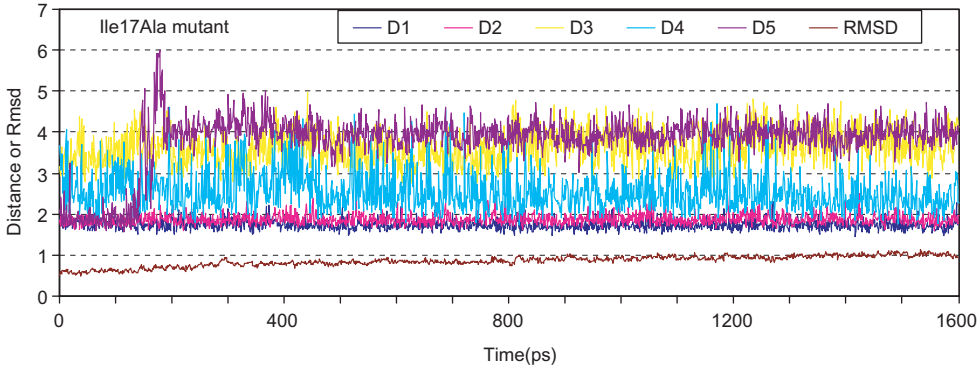

Figure 8. Internuclear distances and C_α trace RMSD during the MD simulation of the Ile17Ala mutant with the ligands. The distances D1 to D5 are depicted in Figure 5. D1 represents the distance between the hydroxyl hydrogen of Thr188 and the phosphate oxygen of NAD^+. D2 refers to the distance between hydrogen of Ile17 backbone NH and the phosphate oxygen of NAD^+. D3 is the distance between oxygen of the sugar group of NAD^+ and nitrogen NZ atom of the amine group of Lys155. D4 represents the distance between the oxygen of the amide group of the nicotinamide ring and the main-chain amine of Val186. D5 is the distance between oxygen of Gln148 amide group and the hydroxyl hydrogen of PGE_2.

600 ps MD simulation, whereas the hydrogen bond (distance D5 in Fig. 8) in the Ile17Ala mutant disappeared after about 150 ps. Further, we superimposed the simulated 15-PGDH–NAD^+–PGE_2 complex for the wild-type protein with that for the Ile17Ala mutant. As shown in Figure 7, the position of NAD^+ in the mutant was shifted slightly to the left side because of the decreased steric hindrance of side chain of the residue 17, resulting in some conformational change of PGE_2 and the increase of distance D5. This is qualitatively consistent with the latest experimental data that the K_m of the Ile17Ala mutant for NAD^+ was about 15-fold larger than that of the wild-type.[13] This further supports that our 3D model of 15-PGDH–NAD^+–PGE_2 complex is reasonable.

Since human 15-PGDH protein is an interesting therapeutic target, identification of the protein binding site for PGE_2 substrate and the 15-PGDH–NAD^+–PGE_2 binding mode is essential for understanding the catalytic mechanism. Making mutations on the identified residues involved in the protein binding with the substrate and testing the catalytic activity of the mutants, one will be able to experimentally examine our computational prediction of the 15-PGDH–NAD^+–PGE_2 binding mode. The 3D model of 15-PGDH–NAD^+–PGE_2 complex obtained from this study might be also useful in future rational design of novel inhibitors of 15-PGDH.

4. Conclusion

The previous studies using site-directed mutagenesis to determine the requirements for productive interaction with the PGE_2 substrate have not been possible to clearly define the domains of the human 15-hydroxyprostaglandin dehydrogenase (15-PGDH) required for the interaction with the PGE2 substrate. In the present study, a combined use of homology modeling, molecular docking, and molecular dynamics simulation techniques led to a 3D model of the entire 15-PGDH–NAD^+–PGE_2 complex. This 3D model shows specific interactions between the NAD^+ cofactor and key amino acid residues in the active site and these interactions are consistent with all of the previously reported experimental data concerning the catalytic activity of 15-PGDH mutants. Our model demonstrates the PGE_2-binding cavity of the protein, which has been unknown. The specific protein-substrate binding mode shown in the model is consistent with previous experimental observation that Ser138, Tyr151, and Lys155 are involved in the catalytic mechanism. Our model further reveals for the first time that Gln148 should also have a role on the catalysis, because its side-chain oxygen atom strongly hydrogen bonds to the hydroxyl group of the substrate.

Acknowledgements

The research was supported in part by the College of Pharmacy and Center for Computational Sciences (CCS) at University of Kentucky.

References and notes

1. Nakano, J.; Anggard, E.; Samuelsson, B. *Eur. J. Biochem.* **1969**, *11*, 386.
2. Thien, F. C.; Walters, E. H. *Prostaglandins Leukot. Essent. Fatty Acids* **1995**, *52*, 271.
3. Ensor, C. M.; Tai, H. H. *J. Lipid Mediators Cell Signal.* **1995**, *12*, 313.
4. Hohl, W.; Stahl, B.; Mundkowski, R.; Hofmann, U.; Meese, C. O.; Kuhlmann, U.; Schlegel, W. *Eur. J. Biochem.* **1993**, *214*, 67.
5. Ensor, C. M.; Yang, J. Y.; Okita, R. T.; Tai, H. H. *J. Biol. Chem.* **1990**, *265*, 14888.
6. Jornvall, H.; Persson, B.; Krook, M.; Atrian, S.; Gonzalez-Duarte, R.; Jeffery, J.; Ghosh, D. *Biochemistry* **1995**, *34*, 6003.
7. Ensor, C. M.; Tai, H. H. *Biochem. Biophys. Res. Commun.* **1991**, *176*, 840.
8. Ensor, C. M.; Tai, H. H. *Biochim. Biophys. Acta* **1994**, *1208*, 151.
9. Ensor, C. M.; Tai, H. H. *Biochem. Biophys. Res. Commun.* **1996**, *220*, 330.
10. Tanaka, N.; Nonaka, T.; Tanabe, T.; Yoshimoto, T.; Tsura, D.; Mitsui, Y. *Biochemistry* **1996**, *35*, 7715.
11. Ensor, C. M.; Tai, H. H. *Arch. Biochem. Biophys.* **1996**, *333*, 117.
12. Zhou, H. P.; Tai, H. H. *Biochem. Biophys. Res. Commun.* **1999**, *257*, 414.
13. Cho, H.; Hamza, A.; Zhan, C.-G.; Tai, H. H. *Arch. Biochem. Biophys.* **2005**, *433*, 447.
14. Krook, M.; Ghosh, D.; Duax, W.; Jornvall, H. *FEBS Lett.* **1993**, *322*, 139.
15. Benson, D. A.; Karsch-Mizrachi, I.; Lipman, D. J.; Ostell, J.; Wheeler, D. L. *Nucleic Acids Res.* **2004**, *32*, D23.
16. Bernstein, F. C.; Koetzle, T. F.; Williams, G. J.; Meyer, E. E., Jr.; Brice, M. D.; Rodgers, J. R., et al. *J. Mol. Biol.* **1977**, *112*, 535.
17. Altschul, S. F.; Gish, W.; Miller, W.; Myers, E. W.; Lipman, D. J. *J. Mol. Biol.* **1990**, *215*, 403.
18. Sogabe, S.; Yoshizumi, A.; Fukami, T.; Shiratori, Y.; Shimizu, S.; Takagi, H.; Nakamori, S.; Wada, M. *J. Biol. Chem.* **2003**, *278*, 19387.
19. Yamashita, A.; Kato, H.; Wakatsuki, S.; Tomizaki, T.; Nakatsu, T.; Nakajima, K.; Hashimoto, T.; Yamada, Y.; Oda, J. *Biochemistry* **1999**, *38*, 7630.
20. Sali, A.; Blundell, T. L. *J. Mol. Biol.* **1990**, *212*, 403.
21. Sali, A.; Blundell, T. L. *J. Mol. Biol.* **1993**, *234*, 779.
22. Laskowski, R. A.; MacArthur, M. W.; Moss, D. S.; Thornton, J. M. *J. Appl. Cryst.* **1993**, *26*, 283.
23. Vriend, G. *J. Mol. Graph.* **1990**, *8*, 52.
24. Frisch, M. J. et al. *Gaussian 03*, Revision A.1; Gaussian, Inc.: Pittsburgh, PA, 2003.
25. Bayly, C. I.; Cieplak, P.; Cornell, W. D.; Kollman, P. *J. Phys. Chem.* **1993**, *97*, 10269.
26. Jorgensen, W. L.; Chandrasekhar, J.; Madura, J. D.; Impey, R. W.; Klein, M. L. *J. Chem. Phys.* **1983**, *79*, 926.
27. Case, D. A.; Pearlman, D. A.; Caldwell, J. W.; Cheatham III, T. E.; Wang, J.; Ross, W. S.; Simmerling, C. L.; Darden, T. A.; Merz, K. M.; Stanton, R. V.; Cheng, A. L.; Vincent, J. J.; Crowley, M.; Tsui, V.; Gohlke, H.; Radmer, R. J.; Duan, Y.; Pitera, J.; Massova, I.; Seibel, G. L.; Singh, U. C.; Weiner, P. K.; Kollman, P. A.AMBER 7, University of California, San Francisco, 2002.
28. Zhan, C.-G.; Zheng, F.; Landry, D. W. *J. Am. Chem. Soc.* **2003**, *125*, 2462.
29. Hamza, A.; Cho, H.; Tai, H.-H.; Zhan, C.-G. *J. Phys. Chem. B* **2005**, *109*, 4776.

30. Zhan, C.-G.; Norberto de Souza, O.; Rittenhouse, R.; Ornstein, R. L. *J. Am. Chem. Soc.* **1999**, *121*, 7279.
31. Koca, J.; Zhan, C.-G.; Rittenhouse, R.; Ornstein, R. L. *J. Am. Chem. Soc.* **2001**, *123*, 817.
32. Koca, J.; Zhan, C.-G.; Rittenhouse, R. C.; Ornstein, R. L. *J. Comput. Chem.* **2003**, *24*, 368.
33. Berendsen, H. J. C.; Postma, J. P. M.; van Gunsteren, W. F.; Di Nola, A. *J. Chem. Phys.* **1984**, *81*, 3684.
34. Ryckaert, J. P.; Ciccotti, G.; Berendsen, H. J. C. *J. Comput. Phys.* **1977**, *23*, 327.
35. Essmann, U.; Perera, L.; Berkowitz, M. L.; Darden, T.; Lee, H.; Pedersen, L. G. *J. Chem. Phys.* **1995**, *103*, 8577.
36. Lin, T. H.; Tsai, K. C.; Lo, T. C. *Protein Eng.* **2003**, *16*, 819.
37. Nevanen, T. K.; Hellman, M. L.; Munck, N.; Wohlfahrt, G.; Koivula, A.; Soderlund, H. *Protein Eng.* **2003**, *16*, 1089.
38. Siqueira, A.; Martins, N. F.; De Lima, M. E.; Diniz, C. R.; Cartier, A.; Brown, D.; Maigret, B. *J. Mol. Graph. Model.* **2002**, *20*, 389.
39. Ghosh, D.; Pletnev, V. Z.; Zhu, D. W.; Wawrzak, Z.; Duax, W. L.; Pangborn, W.; Labrie, F.; Lin, S. X. *Structure* **1995**, *3*, 503.
40. Cho, H.; Oliveira, M. A.; Tai, H. H. *Arch. Biochem. Biophys.* **2003**, *419*, 139.
41. Zhou, H. P.; Yan, F. X.; Tai, H. H. *Eur. J. Biochem.* **2001**, *268*, 3368.
42. Ghosh, D.; Wawrzak, Z.; Weeks, C. M.; Duax, W. L.; Erman, M. *Structure* **1994**, *2*, 629.
43. Breton, R.; Housset, D.; Mazza, C.; Fontecilla-Camps, J. C. *Structure* **1996**, *4*, 905.
44. Oppermann, U. C. T.; Filling, C.; Berndt, D.; Persson, B.; Benach, J.; Ladenstein, R.; Jörnvall, H. *Biochemistry* **1997**, *36*, 34.